PERGAMON

Vision Research 41 (2001) 119–131

Vision Research

www.elsevier.com/locate/visres

M and P retinal ganglion cells of the owl monkey: morphology, size and photoreceptor convergence

Elizabeth S. Yamada [a], Luiz Carlos L. Silveira [a,*], V. Hugh Perry [b], Edna Cristina S. Franco [a]

[a] *Departamento de Fisiologia, Centro de Ciências Biológicas, Universidade Federal do Pará, Pará, 66075-900 Belém, Pará, Brazil*
[b] *School of Biological Sciences, University of Southampton, Southampton SO16 7PX, UK*

Received 15 March 2000; received in revised form 31 July 2000

Abstract

We have estimated photoreceptor convergence to M and P retinal ganglion cells of two closely related nocturnal (owl monkey, *Aotus*) and diurnal (capuchin monkey, *Cebus*) anthropoids. Rod convergence is higher in the owl monkey retina while cone convergence to both M and P cells are very similar in the retinas of the owl monkey and the capuchin monkey. These results indicate that during evolution, the owl monkey retina has undergone changes compatible with a more nocturnal lifestyle, but kept a cone to ganglion cell relation similar to that found in diurnal primates. © 2001 Elsevier Science Ltd. All rights reserved.

Keywords: M and P retinal ganglion cells; Parallel processing; *Aotus*; *Cebus*; Primate

1. Introduction

The retina of the owl monkey shows a number of features consistent with a highly nocturnal lifestyle (Ogden, 1975; Webb & Kaas, 1976; Silveira, Perry, & Yamada, 1993). In comparison to diurnal anthropoids, owl monkeys have fewer cones, more rods and one single class of cones (Wikler & Rakic, 1990; Jacobs, Deegan, Neitz, Crognale, & Neitz, 1993; Jacobs, Neitz, & Neitz, 1996). Owl monkeys have M (midget) and P (parasol) ganglion cells (Silveira, Yamada, Perry, & Picanço-Diniz, 1994), and both cell classes have larger dendritic fields than those of diurnal primates (Yamada, Marshak, Silveira, & Casagrande, 1998). In this paper we determined how dendritic field size of M and P cells in owl monkey changed with retinal eccentricity in relation with rod and cone density. It has been shown that the dendritic field size of M and P cells are correlated with the local cone density, so that cone convergence remains largely unchanged in the central retina but then increases with eccentricity (Goodchild, Ghosh, & Martin, 1996). We investigated whether a similar correlation also holds for the nocturnal owl monkey that has a much lower cone density. Rod convergence was also estimated. For comparison, we quantified cone and rod convergence to M and P cells in the retina of the capuchin monkey, a closely related diurnal primate. In addition, we extended our previous estimates of the M and P cell sizes (Yamada et al., 1998), showing how cell body size and dendritic field size of the inner and outer varieties of these cell classes change across eccentricity. Some of these results have been reported previously in an abstract (Yamada, Silveira, & Perry, 1996a) and a review (Silveira, Yamada, Franco, & Finlay, 2000).

2. Methods

2.1. Animals

Retinas were obtained from 14 adult capuchin monkeys, *Cebus apella*, all males, and seven adult owl monkeys, *Aotus azarae* or *Aotus infulatus*, six males and one female. All animals were provided by the

* Corresponding author. Tel.: +55-91-2111925; fax: +55-91-2111601.
E-mail address: luiz@ufpa.br (L.C.L. Silveira).

0042-6989/01/$ - see front matter
PII: S0042-6989(00)00244-3

Centro Nacional de Primatas (CENP, Ananindeua, Pará, Brazil).

2.2. Optic nerve deposit of Biocytin

We performed all experiments observing the NIH Guidelines regarding the care and use of animals for experimental procedures. Surgical procedures were carried out under aseptic conditions and keeping the animal deeply anaesthetised. A 1:4 anaesthetic mixture of 2% xylidine–tiazine chlorhydrate solution, Rompun (Bayer, São Paulo, SP, Brazil) and 5% ketamine chlorhydrate solution, Ketalar (Parke–Davis, Guarulhos, SP, Brazil), 0.5–1.0 ml/kg intramuscular, was used at 1–2 h intervals. The methods have been fully described elsewhere (e.g. Yamada, Silveira, & Perry, 1996b). In brief, animals were deeply anaesthetised and placed in a stereotaxic apparatus. During the surgical procedure, normal body temperature was maintained and the electrocardiogram monitored. The optic nerve was exposed through a dorsolateral opening of the bony orbit and small pieces of gelfoam that had been previously saturated in a 35% Biocytin (Sigma, St. Louis, MO) solution were placed within a longitudinal cut made in the nerve 1–3 mm behind the eye. A piece of cellophane was positioned on the lesion and sealed with glue to prevent tissue fluid washing out the tracer. After 24–48 h survival time, the animal was euthanised with a lethal dose of Thionembutal (Abbot, São Paulo, SP, Brazil), and perfused through the ascending aorta with 0.9% buffered saline solution followed by 1–4% phosphate-buffered paraformaldehyde. Next, the eye was removed and the retina dissected free in a chilled solution of the same fixative. After removing the vitreous, the retina was immersed in 0.01% collagenase (Boehringer–Mannhein, Mannhein, Germany) solution for 1–5 min, returned to fixative for 5 min, and then washed for 0.5–1 h in phosphate buffer (0.1 M, pH = 7.2–7.4). The retina was pre-incubated in avidin–biotin-peroxidase solution (ABC Vectastain Standard Kit, Vector Laboratories, Burlingame, CA) for 24–48 h, and the reaction product was developed using a nickel-enhanced glucose oxidase method, with diaminobenzidine tetrahydrochloride (Sigma) as the chromogen. To enhance the contrast of labelled profiles against the background, the retina was immersed in a 0.1% osmium tetroxide solution for 1 min. After washing in phosphate buffer for 30–60 min, the retina was mounted on a gelatinised slide, covered with a piece of filter paper and a clean slide, and immersed for 12 h in 1:9 formalin/ethanol solution. In the following day, the retina was dehydrated, cleared, and coverslipped using DPX (BDH Laboratory Supplies, Poole, UK) as the mounting medium.

2.3. Ganglion cell analysis

Dendritic field and soma size measurements from capuchins cells were those published previously, and comprised 264 M and 419 P ganglion cells selected from four well-labelled capuchin retinas (Yamada et al., 1996b). Owl monkey cells were sampled in seven retinas and comprised 239 M and 257 P ganglion cells, including those studied previously (Yamada et al., 1998) plus a new group of centrally located cells.

M and P retinal ganglion cells were identified by the morphological features described previously (Perry, Oehler, & Cowey, 1984; Watanabe & Rodieck, 1989; Silveira et al., 1994). Soma and dendritic field outlines were drawn using a camera lucida attached to a binocular microscope Nikon Labophot-2 (Garden City, NY). All drawings were made under $\times 100$ oil immersion objective giving a final magnification of $\times 1500$. Cells were selected within a two 45° sectors, one temporal and the other nasal to the fovea, centred on the horizontal meridian, which was defined as a straight line intersecting the fovea and the optic disc. In some owl monkey retinas, an area centralis, not a fovea, was present; the centre of the area centralis was used as a reference in those cases. The sizes of cell bodies and dendritic fields were expressed either as the area or the diameter of a circle of the same size, and retinal eccentricities measured from the centre of the fovea or area. Prior to dehydration the distance between the fovea (or area) and the centre of the optic disk was 3.6 ± 0.1 mm. Correction for shrinkage of eccentricity values was applied when this distance after dehydration was less than 3.5 mm.

2.4. Cone and rod spatial densities

We estimated cone and rod spatial densities in three owl monkey retinas and seven capuchin monkey retinas. Counts were made along the horizontal meridian, and were performed with a binocular microscope under $\times 100$ oil immersion objective. In the central region, sampled regions were located at 0, 0.05, 0.1, 0.25, 0.5 and 0.75 mm from fovea. From 1 mm towards the periphery, counts were made every 1 mm. For cone counts, the sampled areas were: 256 μm^2 between 0 and 0.1 mm; 1024 μm^2 between 0.25 and 1 mm; and 6400 μm^2 from distances 2 mm of the fovea. For rod counts, a single sampling area of 1024 μm^2 was used for all locations.

Cone and rod convergence to retinal ganglion cells were calculated as described in Goodchild et al. (1996). We multiplied the dendritic field area of M or P cells by the cone or rod density at each eccentricity to obtain the number of cones or rods per ganglion cell. These values of cone or rod convergence were plotted as a function of retinal eccentricity.

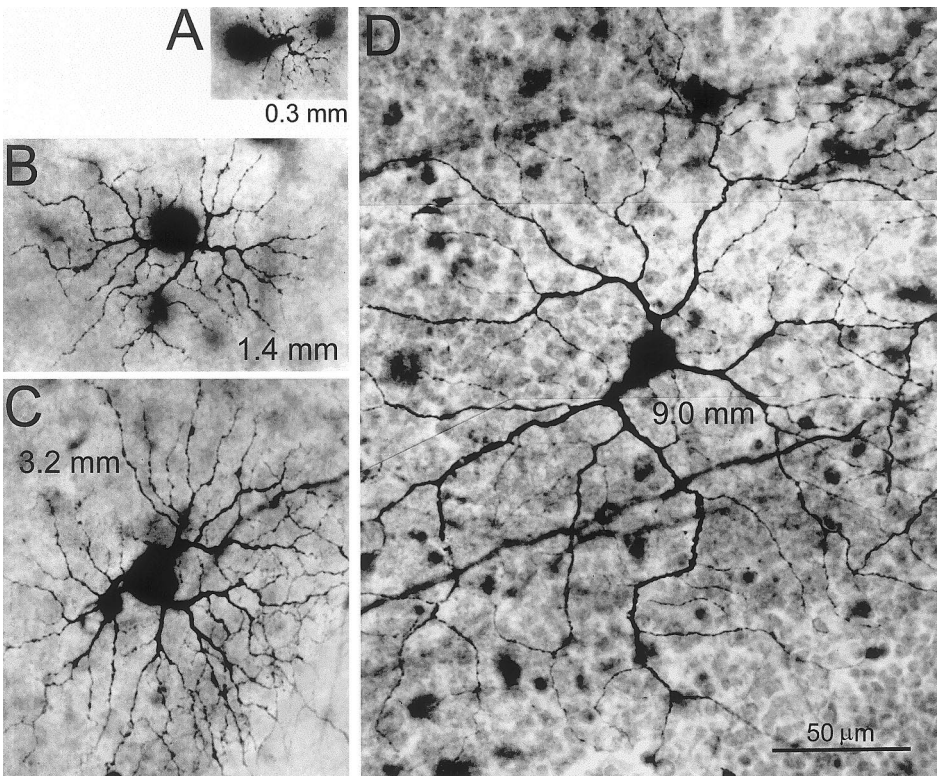

Fig. 1. Photomicrographs of M ganglion cells of the owl monkey retina. The cells were retrogradely labelled from optic nerve deposits of Biocytin. M cells were situated at different retinal eccentricities, given in the figure. Scale bar in D applies to all panels.

3. Results

3.1. Owl monkey retinal ganglion cells

Distinct classes of retinal ganglion cells were filled over large regions of each retina. We classified owl monkey ganglion cells using morphological criteria reported previously for diurnal anthropoids. These criteria derived from studies that used retinal preparations stained by a variety of methods such as retrograde labelling with horseradish peroxidase (Leventhal, Rodieck, & Dreher, 1981; Perry et al., 1984), intracellular injection of Lucifer Yellow or Neurobiotin (Watanabe & Rodieck, 1989; Dacey & Petersen, 1992), and the method of Golgi (Polyak, 1941; Boycott & Dowling, 1969; Rodieck, Binmoeller, & Dineen, 1985; Kolb, Lindberg, & Fisher, 1992). The quality of dendritic filling using retrograde transport of Biocytin is comparable with that obtained using the above methods.

The photomicrographs of Figs. 1 and 2 illustrate the distinct morphology of M and P ganglion cells of the owl monkey retina at different retinal eccentricities. In the owl monkey, as in other species, the knowledge of eccentricity is essential when classifying cell types. M ganglion cells (Fig. 1) have large somata, thick axons, and large and radiate dendritic trees. In the central retinal region, M cells usually have one or two primary dendrites, while towards the retinal periphery they exhibit three or four thick primary dendrites. On the other hand, P ganglion cells (Fig. 2) have small somata, thin axons and small, tortuously branched dendritic trees. In the central region, P cells exhibit one

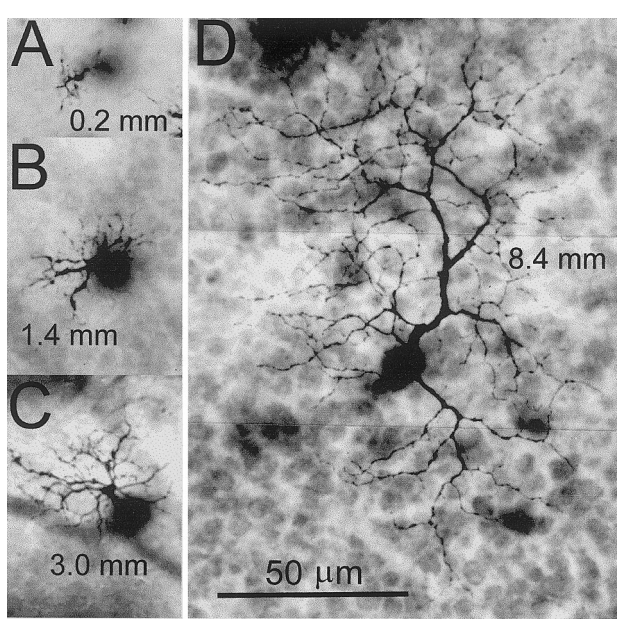

Fig. 2. Photomicrographs of P ganglion cells of the owl monkey retina. The cells were retrogradely labelled from optic nerve deposits of Biocytin. P cells were situated at comparable eccentricities as the M cells depicted in the Fig. 1. Scale bar in D applies to all panels.

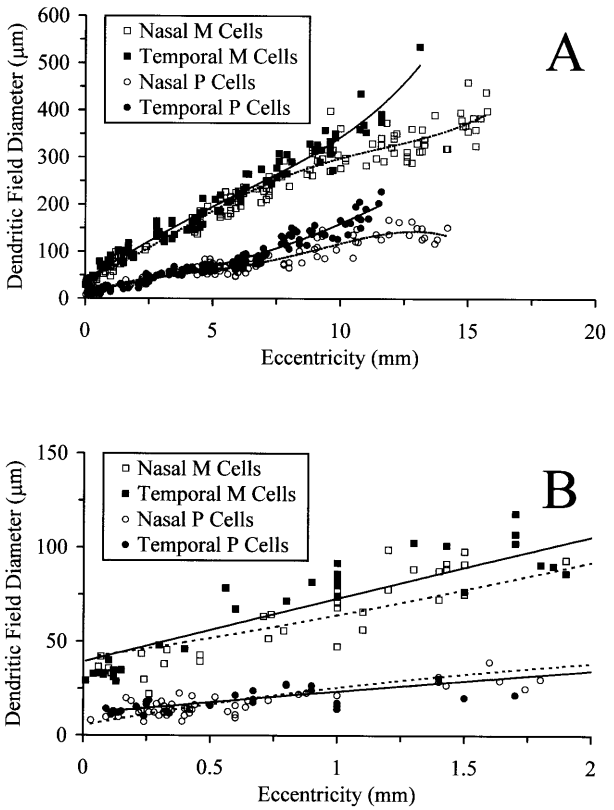

Fig. 3. Dendritic field diameters of M and P ganglion cells of the owl monkey retina: a comparison between temporal and nasal retinas. M cells are represented as squares and P cells as circles. For both M and P cells, dendritic field diameters increase less steeply along the nasal retina (empty symbols) in comparison to the temporal retina (filled symbols). The solid and dashed lines are fourth order polynomial functions best fit to the data points. (A) M and P cells that were labelled along the entire horizontal meridian. (B) M and P cells of central retinal region along the horizontal meridian.

primary dendrite, while towards the retinal periphery, P cells with either one or two primary dendrites are found. Figs. 3 and 4 show how dendritic field sizes and cell body sizes of M and P cells change along the horizontal meridian. In these, and in the next figures, we have distinguished with different symbols cells located in the nasal or temporal sides of the retina. Table 1 shows the statistical analysis for the sizes of M and P cells located in some representative retinal regions. M cells have larger dendritic fields and cell bodies than P cells both in the central and peripheral retinal regions. The dendritic field diameters of M cells are much larger than those of P cells from the same retinal locations, and the difference between these two cell classes remains more or less constant along the horizontal meridian, M cell dendritic fields being 2.3–2.7 times larger than those of P cells. The difference is small for cell body diameters, M cell bodies being only 1.1–1.2 times larger than those of P cells in the central region and 1.4–1.5 times larger in the retinal periphery.

Other ganglion cell morphologies were also observed in the owl monkey retina. They all resembled wide-field ganglion cells of the macaque and human retina, that project to the superior colliculus, pretectum, and LGN koniocellular layers (Perry & Cowey, 1984; Kolb et al., 1992; Rodieck & Watanabe, 1993; Peterson & Dacey, 1999; Solomon, White, & Martin, 1999). On the other hand, in contrary to our previous statement in Silveira et al. (1994), we have not found small-field bistratified ganglion cells in the owl monkey retina.

3.2. Dendritic field and soma sizes of nasal and temporal M and P cells of the owl monkey retina

Fig. 3 shows that for most of the horizontal meridian, as far as 5 mm from the fovea, M or P cells located nasal to the fovea have dendritic fields similar in size to their temporal counterparts; towards retinal periphery, temporal cells tend to have larger dendritic fields than nasal cells of the same class. For cell body size, there is an even larger overlap between nasal and temporal cells (Fig. 4). There are no significant differences in cell body and dendritic field sizes between nasal and temporal cells of the same class located close to the fovea (≤ 0.5 mm). In the retinal periphery, for distances from fovea ≥ 10 mm, these differences attain the significant level for both cell body size and dendritic field size, temporal cells being larger than nasal cells of the same class.

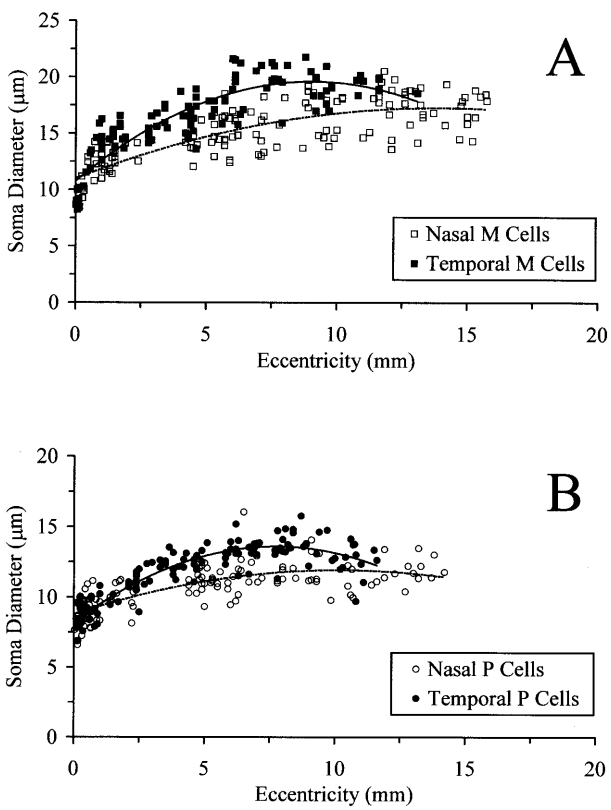

Fig. 4. Soma diameters of M and P ganglion cells of the owl monkey retina. (A) Temporal and nasal M cells. (B) Temporal and nasal P cells. The solid and dashed lines are second order polynomial functions best fit to the data.

Table 1
Owl monkey M and P ganglion cells: dendritic field and cell body diameter for cells located in the central and peripheral retinal regions

Retinal region or comparison	Distance from fovea (mm)	Cell class	Dendritic field diameter (μm)	Student t test, two-tail (P value)	Cell body diameter (μm)	Student t test, two-tail (P value)
Nasal	≤0.5	M cells ($N=11$)	37 ± 7		10.2 ± 1.4	
Temporal	≤0.5	M cells ($N=13$)	35 ± 6		9.4 ± 1.0	
Nasal	≤0.5	P cells ($N=34$)	14 ± 4		8.8 ± 0.8	
Temporal	≤0.5	P cells ($N=13$)	14 ± 3		8.5 ± 1.0	
M cells (Nas × Tem)	≤0.5			>0.1 (n.s.)		>0.1 (n.s.)
P cells (Nas × Tem)	≤0.5			>0.5 (n.s)		>0.1 (n.s.)
Nasal cells (M × P)	≤0.5			<0.0001		<0.05
Temp. cells (M × P)	≤0.5			<0.0001		<0.05
Nasal	≥13	M cells ($N=21$)	363 ± 40		17 ± 2	
Nasal	≥10	M cells ($N=43$)	340 ± 41		17 ± 2	
Temporal	≥10	M cells ($N=8$)	401 ± 60		19 ± 1	
Nasal	≥13	P cells ($N=7$)	136 ± 14		12 ± 1	
Nasal	≥10	P cells ($N=19$)	136 ± 20		12 ± 1	
Temporal	≥10	P cells ($N=13$)	178 ± 26		13 ± 1	
M cells (Nas × Tem)	≥10			<0.05		<0.0001
P cells (Nas × Tem)	≥10			<0.0001		<0.05
Nasal cells (M × P)	≥13			<0.0001		<0.0001
Temp. cells (M × P)	≥10			<0.0001		<0.0001

3.3. Dendritic field and soma sizes of the inner and outer varieties of owl monkey M and P cells

An asymmetry in dendritic field size between inner and outer varieties of M and P ganglion cells has been described in human, macaque and marmoset retina (Dacey & Petersen, 1992; Dacey, 1993; Ghosh, Goodchild, Sefton, & Martin, 1996). A small asymmetry is also found in the periphery of the capuchin monkey retina (Yamada et al., 1996b). According to those authors, inner M and P cells have larger dendritic trees than their outer counterparts. To determine whether the same was true for the owl monkey retina, we measured the dendritic field diameters of inner and outer stratifying M and P cells. The depth of stratification was determined by observing the focus plane of the dendrites in the inner plexiform layer. The results for the horizontal meridian are shown in Fig. 5. There is a tendency for outer P cells to have larger dendritic fields thant inner P cells, both in the temporal and nasal regions; there are no obvious differences for M cell. We tested if inner and outer cells were different in sizes for in central and peripheral regions separately, and the results are shown in Table 2. As could be predicted from Fig. 5, outer P cells have larger dendritic fields than inner P cells, both in the centre and periphery, and also for nasal and temporal regions, but there are no consistent differences between inner and outer M cells. Our results showed an inner-to-outer asymmetry for the P cells of the owl monkey retina that is the opposite of the one described for human, macaque and marmoset. Our results thus predict that in the owl monkey, P cells giving OFF light responses should have, on average, larger receptive fields than ON-cells.

Table 2 also shows the results for cell body size comparison. In some regions, mostly in the retinal periphery, there are differences for both M and P cells, but in those cases inner cells have larger cell bodies than outer cells. These results for soma sizes are similar to those previously reported for M cells that were obtained from owl monkey retinas stained by the Gros–Schultze neurofibrillar method (Lima, Silveira, & Perry, 1996).

3.4. A comparison with a diurnal New World monkey

In Fig. 6A and B we compare owl monkey ganglion cells with those of the capuchin monkey. Data for

capuchin monkey was taken from Yamada et al. (1996b). The owl monkey and the capuchin monkey are phylogenetically closely related and their retinas are of similar extent (Silveira, Picanço-Diniz, Sampaio, & Oswaldo-Cruz, 1989; Silveira et al., 1993). In the capuchin monkey retina, because of the foveal pit, retinal ganglion cells are laterally displaced. The magnitude of the displacement depends on the length of the Henle fibres and on the bipolar cell displacement. These values are not known for the capuchin monkey retina. Thus, to correct for the central displacement of the retinal ganglion cells in this primate we applied the following polynomial equation used for the same purposes in the retina of the crab-eating macaque (*Macaca fascicularis*) (Goodchild et al., 1996):

$$y = -0.0266x^2 + 1.248x - 0.599 \quad (1)$$

where y is eccentricity corrected for lateral displacement and x is uncorrected eccentricity. This equation should give a good approximation, because capuchin monkey retina has approximately the same dimensions and ganglion cell density as the retina of the crab-eating macaque (Silveira et al., 1989; Wässle, Grünert, Röhrenbeck, & Boycott, 1990). The equation was used to correct cell eccentricity for the central 3 mm from fovea in the capuchin monkey retina, so that the dendritic field area could be related to the photoreceptor density (see below). Because the central displacement of retinal ganglion cells is small or negligible in the owl monkey (Jones, 1965; Ogden, 1974), we chose not to apply any correction for displacement in the retina of this primate.

Fig. 6 shows dendritic field areas of M and P cells in the owl monkey (filled symbols) and the capuchin monkey retina (empty symbols), for both temporal (A) and nasal (B) regions. Data plotted in this figure were means and standard deviations taken from cells located at 1 mm intervals whose midpoint is indicated in the abscissa. For the capuchin monkey, values were plotted after correction for central displacement of cells located in the central 3 mm from fovea. In comparison to capuchin monkey, owl monkey M cells are larger all across the retina. The owl monkey/capuchin monkey ratio for the dendritic field area of M cells is 3.6–4.1 at 0.5 mm from the fovea, decreasing towards retinal periphery to 1.4–2.3 at 12 mm of eccentricity. Owl monkey P cells are also larger than their counterparts in the capuchin monkey retina all across the retina. The

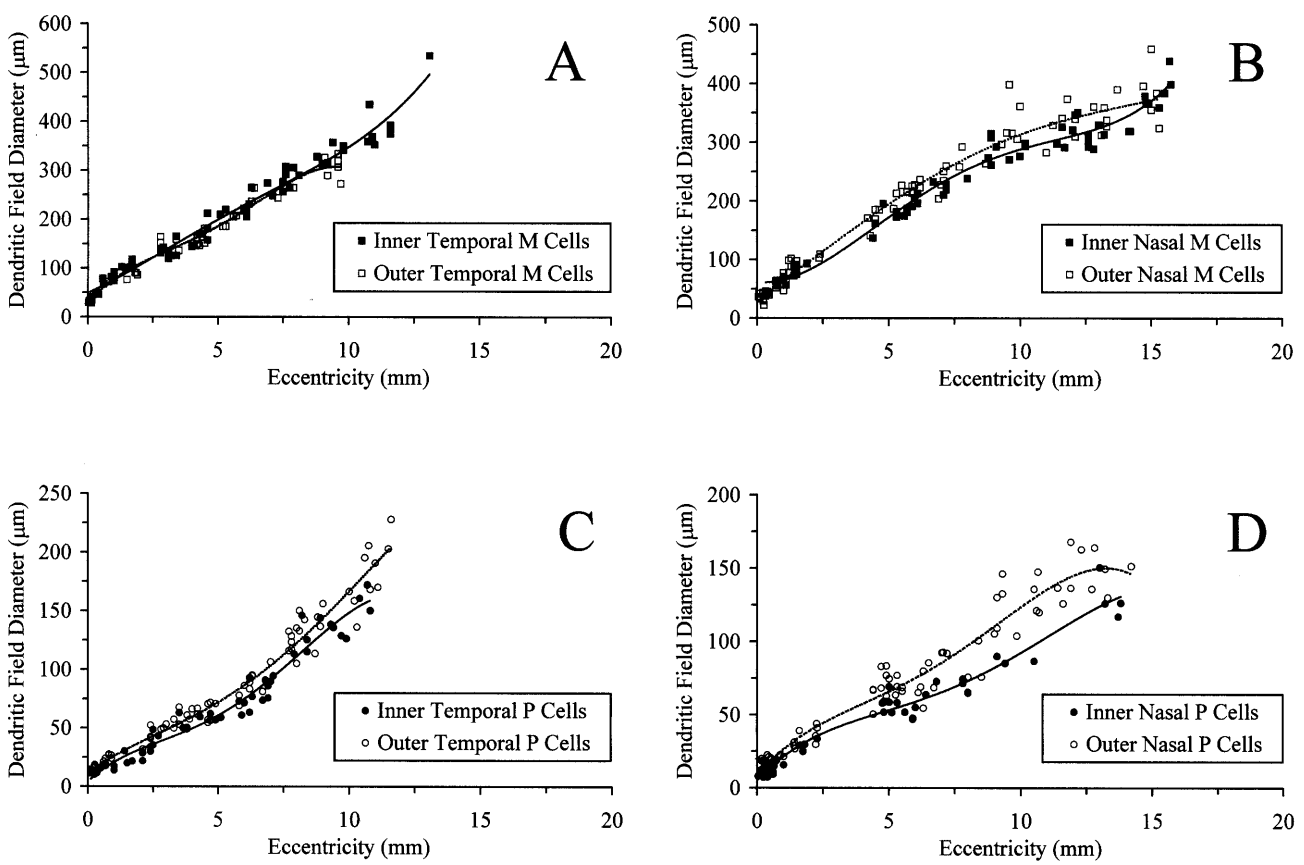

Fig. 5. Dendritic field diameters of inner and outer stratifying M and P ganglion cells of the owl monkey retina. Inner cells are represented as filled symbols and outer cells as empty symbols. (A) Temporal M cells. (B) Nasal M cells. (C) Temporal P cells. (D) Nasal P cells. The solid and dashed lines are fourth order polynomial functions best fit to the data.

Table 2
Owl monkey M and P ganglion cells of the inner and outer varieties: dendritic field and cell body diameter for cells located in the central and peripheral retinal regions

Retinal region or comparison	Distance from fovea (mm)	Cell class	Dendritic field diameter (μm)	Student t test, two-tail (P value)	Cell body diameter (μm)	Student t test, two-tail (P value)
Nasal	≤1	M_{in} cells ($N=6$)	57 ± 11		11.9 ± 1.2	
Nasal	≤1	M_{out} cells ($N=13$)	43 ± 15		10.7 ± 1.8	
Nasal cells $M_{in} \times M_{out}$	≤1			<0.05		0.1
Nasal	≥5	M_{in} cells ($N=46$)	280 ± 69		17.7 ± 1.2	
Nasal	≥5	M_{out} cells ($N=42$)	297 ± 66		14.9 ± 1.5	
Nasal cells $M_{in} \times M_{out}$	≥5			>0.1 (n.s.)		<0.0001
Temporal	≤1	M_{in} cells ($N=12$)	63 ± 22		12.7 ± 2.5	
Temporal	≤1	M_{out} cells ($N=12$)	48 ± 23		10.3 ± 2.2	
Temp. cells $M_{in} \times M_{out}$	≤1			>0.1 (n.s.)		<0.05
Temporal	5–10	M_{in} cells ($N=23$)	274 ± 48		20.0 ± 1.2	
Temporal	5–10	M_{out} cells ($N=15$)	258 ± 50		17.4 ± 1.4	
Temp. cells $M_{in} \times M_{out}$	5–10			>0.1 (n.s.)		<0.0001
Nasal	≤1	P_{in} cells ($N=20$)	12 ± 3		8.9 ± 1.0	
Nasal	≤1	P_{out} cells ($N=26$)	16 ± 4		8.9 ± 0.9	
Nasal cells $P_{in} \times P_{out}$	≤1			<0.005		>0.5 (n.s.)
Nasal	≥5	P_{in} cells ($N=22$)	77 ± 29		11.8 ± 1.0	
Nasal	≥5	P_{out} cells ($N=38$)	108 ± 34		11.4 ± 1.3	
Nasal cells $P_{in} \times P_{out}$	≥5			<0.001		>0.1 (n.s.)
Temporal	≤1	P_{in} cells ($N=6$)	15 ± 3		9.6 ± 1.1	
Temporal	≤1	P_{out} cells ($N=17$)	18 ± 6		8.6 ± 0.9	
Temp. cells $P_{in} \times P_{out}$	≤1			<0.05		<0.1
Temporal	≥5	P_{in} cells ($N=25$)	107 ± 34		13.7 ± 0.7	
Temporal	≥5	P_{out} cells ($N=33$)	135 ± 41		13.0 ± 1.2	
Temp. cells $P_{in} \times P_{out}$	≥5			<0.01		<0.01

owl monkey/capuchin monkey ratio for the dendritic field area of P cells is 5.9 at 0.5 mm from the fovea and 3–4 in the retinal periphery.

3.5. Cone and rod convergence to M and P cells

Fig. 6C and D shows how cone and rod density changes as a function of eccentricity along the horizontal meridian for the retinas of the owl monkey and capuchin monkey, respectively. In the fovea of the owl monkey (Fig. 6C), cone density was $16\,300 \pm 2800$/mm^2 and rod density was $388\,000 \pm 103\,500$/mm^2. Towards the retinal periphery, cone density drops to 4500 and 3000 cones/mm^2 in the nasal and temporal sides of the horizontal meridian, respectively, whilst rod density drops to 175 000 and 120 000 rods/mm^2, in the same regions. Our results for the owl monkey retina (Fig. 6C) are similar to those of Ogden (1975) and Wikler and Rakic (1990) except that we found higher values for cone density in the central retinal region. We have used a different anatomical preparation than Ogden. Also, we used a smaller sampling interval than Wikler and Rakic (1990), which provided a better peak density resolution.

For capuchin monkey retina (Fig. 6D), cone density has a value of $162\,100 \pm 15\,100$ cones/mm^2 in the centre of the fovea. Rods were absent in the very centre of the fovea and the highest values occurred in a ring at 3–6 mm of eccentricity. The rod density peak was $138\,000 \pm 15\,000$ rods/mm^2 at 6 mm nasal to the fovea. Along the nasotemporal meridian, the photoreceptor density drops to 7500 cones/mm^2 and 68 700 rods/mm^2 in the nasal periphery and 6250 cones/mm^2 and 77 800 rods/mm^2 in the temporal periphery.

In Fig. 7, we plotted the cone and rod convergence to M and P cells in the owl monkey and the capuchin monkey. The dendritic field area values were the same as plotted in Fig. 6A–B and photoreceptor density values were those from Fig. 6C–D. The results show that the owl monkey and capuchin monkey have about the same cone convergence to M and P cells all along the horizontal meridian (Fig. 7A–B). On the other hand, also along the horizontal meridian, the owl monkey has larger rod convergence to both M and P cells than the capuchin monkey (Fig. 7C and D).

In the owl monkey retina, rod convergence to M cells is 410 rods/cell in the fovea. It increases along the horizontal meridian from 1600 to 2100 at 1 mm from fovea to 13 900–16 200 rods/cell at the retinal periphery. In the capuchin monkey retina, rod convergence to M cells is much lower. It ranges along the horizontal meridian from 70 to 80 rods/cell at 1 mm from the fovea to 4700–6500 rods/cell at the retinal periphery. In the owl monkey retina, rod convergence to P cells is also high. It varies from 60 rods/cell in the fovea, increasing along the horizontal meridian from 110 to 130 rods/cell at 1 mm from fovea to 2400–4400 rods/cell at the retinal periphery. On the other hand, in the capuchin monkey retina, rod convergence to P cells is much lower, ranging from 4 to 7 rods/cell at 1 mm from the fovea to 570–880 rods/cells at the retinal periphery.

Cone convergence to M and P cells is similar for the owl monkey and capuchin monkey. In the owl monkey retina, cone convergence to M cells is 17 cones/cell in the fovea, increasing from 40 to 50 cones/cell at 1 mm from fovea to 340–420 cones/cell at the retinal periphery. In the capuchin monkey retina, cone convergence to M cells varies from 20 cones/cell at 1 mm of distance from fovea to 500 cones/cell at the retinal periphery. Cone convergence to P cells also has a similar range of values for the owl monkey and capuchin monkey reti-

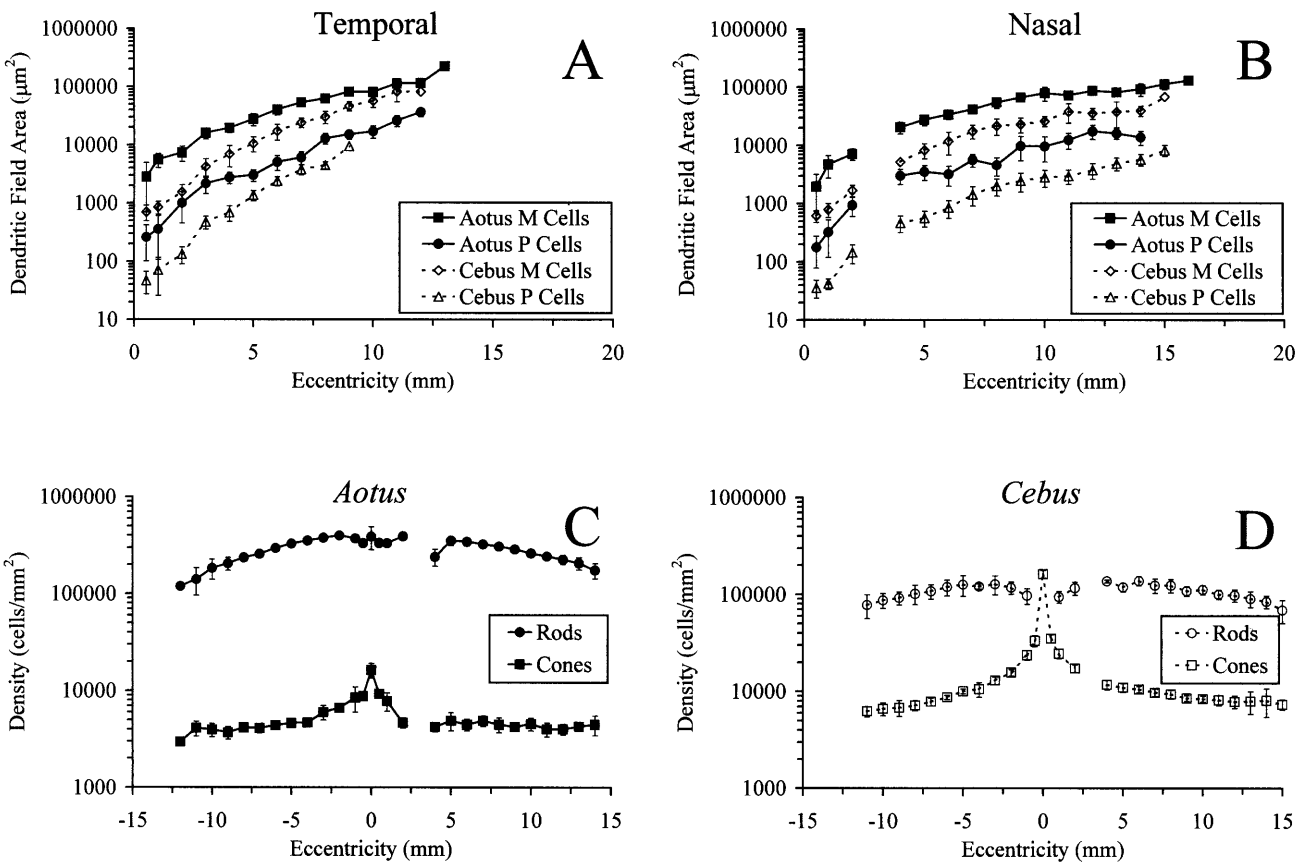

Fig. 6. Comparison between the retina of two closely related anthropoids, the diurnal capuchin monkey (*Cebus*, empty symbols) and the nocturnal owl monkey (*Aotus*, closed symbols): M and P dendritic field size (A–B) and photoreceptor density (C–D). (A) Dendritic field areas of M and P cells as a function of temporal eccentricity for the owl monkey and capuchin monkey. (B) Dendritic field areas of M and P cells as a function of nasal eccentricity for the owl monkey and capuchin monkey. (C) Photoreceptor densities as a function of retinal eccentricity for the retina of the owl monkey. (D) Photoreceptor densities as a function of retinal eccentricity for the retina of the capuchin monkey. For (C–D) nasal and temporal eccentricities are represented by positive and negative values, respectively. For (A–D) symbols and bars are means and standard deviations. When the bar is not represented the standard deviation was smaller than the symbol size.

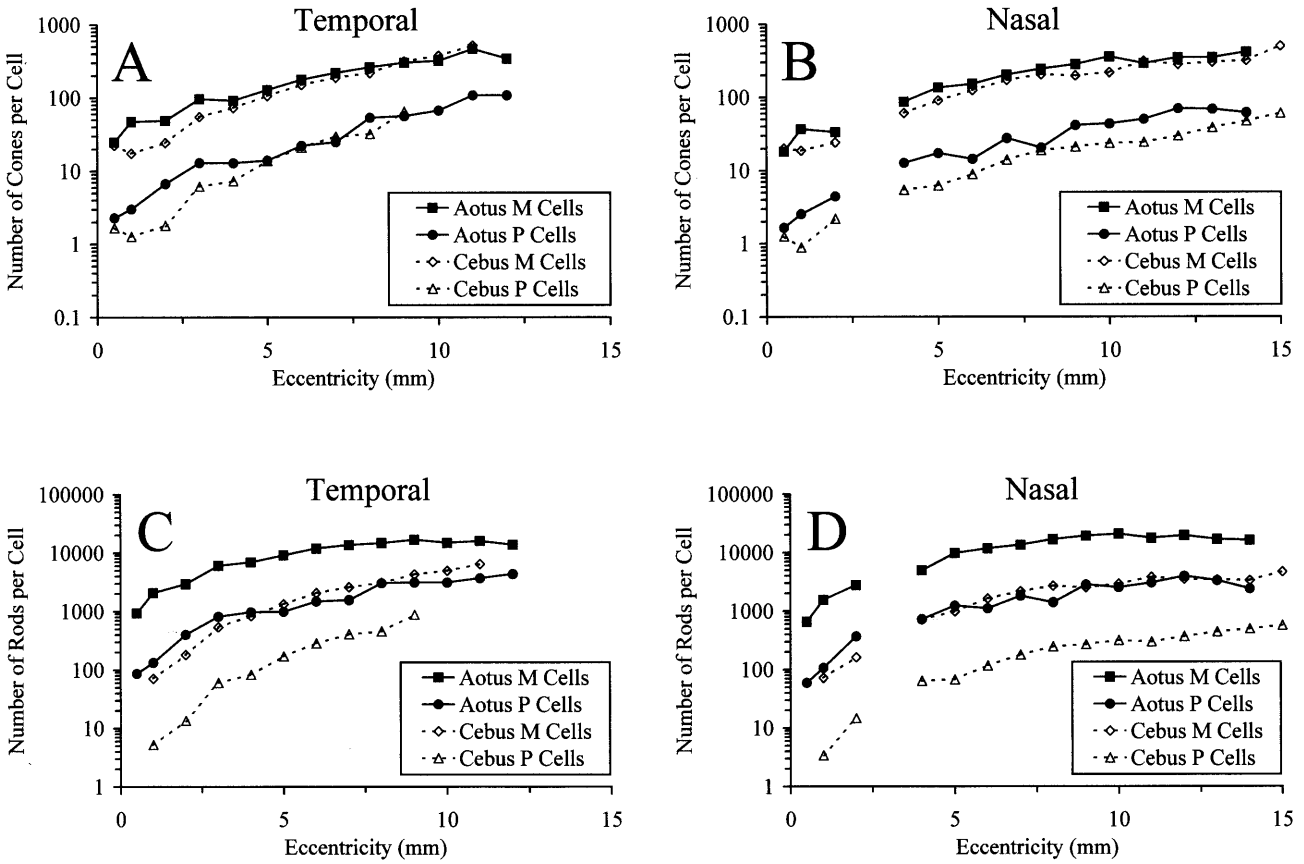

Fig. 7. Photoreceptor convergence to M and P ganglion cells as a function of retinal eccentricity. In all plots, data from the owl monkey retina (represented as filled symbols) are compared with those from the capuchin monkey retina (represented as empty symbols). (A) Cone convergence to M and P cells in the temporal side of the horizontal meridian. (B) Cone convergence to M and P cells in the nasal side of the horizontal meridian. (C) Rod convergence to M and P cells in the temporal horizontal meridian. (D) Rod convergence to M and P cells in the nasal horizontal meridian. Cone and rod convergence were obtained by multiplying the dendritic field area of M or P cells (Fig. 6A and B) by the cone or rod densities (Fig. 6C and D) to obtain number of cones or rods per ganglion cell.

nas. In the owl monkey retina, cone convergence to P cells is 2.5 cones/cell in the fovea, increasing from 2.5 to 3 cones/cell at 1 mm from fovea to 60–110 cones/cell at the retinal periphery. In the capuchin monkey retina, cone convergence to P cells varies from 1 to 2 cones/cell at 1 mm of distance from fovea to 60 cones/cell at the retinal periphery. These values of cone convergence are in the same range as those reported for M and P cells in other primates (Goodchild et al., 1996).

4. Discussion

4.1. The M and P pathways in the owl monkey: physiological considerations

The owl monkey has well-defined magno- and parvocellular layers in the LGN (Kaas, Huerta, Weber, & Harting, 1978; Kaas & Huerta, 1988) and the projection patterns of these LGN neurones to the primary visual cortex are similar to those of other primates (Casagrande & Kaas, 1994). A direct demonstration that the M and P cells described here do indeed project to the magno- and parvocellular layers of the LGN is still lacking. However, that is very plausible, given that our classification was based on the their morphological similarity to the M and P ganglion cells described in other primates in which this projection has already been demonstrated (Leventhal et al., 1981; Perry et al., 1984; Watanabe & Rodieck, 1989). Moreover, some of the morphological features described for the M and P cells in our study are consistent with response properties previously reported for owl monkey LGN magno- and parvocellular neurones. It has been reported that LGN magnocellular cells have receptive field centre diameter 1.5–3 times larger than parvocellular cells, and that LGN magnocellular cells have shorter latencies to orthodromic optic chiasm stimulation then LGN parvocellular cells (Sherman, Wilson, Kaas, & Webb, 1976; O'Keefe, Levitt, Kiper, Shapley, & Movshon, 1998; Usrey & Reid, 2000). These two physiological properties agree with our morphological findings that dendritic field diameters of M cells are two to threefold larger than those of P cells, and that M cells have larger somas and thicker axons than P cells.

The owl monkey M pathway shares many similarities with that of diurnal monkeys. Owl monkey LGN magnocellular neurones are broad-band, transient and have large receptive fields (Jones, 1966; Sherman et al., 1976; O'Keefe et al., 1998; Usrey & Reid, 2000) as retinal and LGN neurones of diurnal anthropoids (Wiesel & Hubel, 1966; Gouras, 1968; de Monasterio & Gouras, 1975; Kaplan & Shapley, 1982; Lee, Martin, & Valberg, 1988; Croner & Kaplan, 1995; Yeh, Lee, Kremers, Cowing, Hunt, Martin, & Troy, 1995; Kremers & Weiss, 1997; Kremers, Weiss, Zrenner, & Maurer, 1997; Lee et al., 2000; Usrey & Reid). The M pathway in Old World primates is likely to support a luminance channel with little role in chromatic vision (Lee et al., 1988; Kaplan, Lee, & Shapley, 1990; Solomon et al., 1999). There is also evidence from macaque monkey studies that the M pathway (Purpura, Kaplan, & Shapley, 1988) mainly mediates pattern vision at scotopic levels. It is interesting that the nocturnal owl monkey has a higher proportion of M ganglion cells, 15% (Lima et al., 1996), and has a higher rod convergence to both M and P ganglion cells (present study) in comparison with diurnal monkeys. Since both features would increase sensitivity at low luminance levels, it may be supposed that both of them represent adaptations to nocturnal habits.

Only broadband units have been recorded from both magno- and parvocellular layers of the owl monkey LGN (Jones, 1966), and this is consistent with more recent anatomical and physiological studies which have shown that the owl monkey has only one cone type (Wikler & Rakic, 1990; Jacobs et al., 1993). Thus, the P pathway in the owl monkey is 'colour blind', with neurones showing broadband spectral responses similar to those of the M pathway. In this regard, LGN P pathway neurones of the owl monkey are functionally different from those of diurnal trichromatic primates. However, the sustained character of their light response and their smaller receptive fields are some of the properties common to P pathways in both diurnal and nocturnal monkeys (Sherman et al., 1976; O'Keefe et al., 1998; Usrey & Reid, 2000). Moreover, the lack of spectral response of the neurones of the owl monkey P pathway would per se not rule them out as being homologues of those of diurnal monkeys. It has now been shown that diurnal dichromatic primates, such as male capuchin monkeys, squirrel monkeys and marmosets, also have P ganglion cells and LGN parvocellular neurones which, apart from the lack of colour-opponence, exhibit response properties very similar to colour-opponent P cells of trichromatic New- and Old World primates, including low luminance contrast sensitivity (Yeh et al., 1995; Kremers & Weiss, 1997; Kremers et al., 1997; Lee, Silveira, Yamada, Hunt, Kremers, Martin et al., 2000; Usrey & Reid, 2000). Therefore, it seems reasonable to suppose that the P pathway is not intrinsically different in diurnal and nocturnal simians.

4.2. Spatial sampling by the cone and ganglion cell mosaics in the owl monkey retina

Behavioural visual acuity of the owl monkey is 7.5–10 cpd (Ordy & Samorajski, 1968; Jacobs, 1977). In humans, the psychophysical grating resolution of 50–60 cpd matches the frequency resolution of the foveal cone mosaic (Rowe, 1991). To determine whether the same was true for the owl monkey, we estimated the sampling characteristics of the foveal cone array based on our estimate of peak cone density. Assuming a hexagonal mosaic (Peichl & Wässle, 1979), the intercone spacing d, in μm, can be estimated using the following equation:

$$d = ((1/D)(2/3)^{0.5})1000 \quad (2)$$

where D is cell density in cell/mm^2. Using $D = 16\,300$ cones/mm^2, we estimated an intercone spacing of 8.4 μm.

To determine the spatial resolution limit imposed by the intercone spacing, the retinal magnification factor (RMF) must be taken into account. In the owl monkey, the cortical representation for the horizontal meridian in the temporal visual field occupies $\sim 100°$ (Allman & Kaas, 1971). In our preparations the mean value for the retinal nasal meridian was 17 mm. This gives an RMF of 170 m/deg. We took this value as the mean RMF, that is, the RMF at 50° of visual angle. Given that for other primates (human, macaque and capuchin monkey), the RMF in the foveal region is $\sim 15\%$ higher than the value at 50°, and assuming that the same is also true for *Aotus*, we estimated a foveal RMF of 200 μm/deg. We used the following equation to calculate the spatial resolution limit N_f, the Nyquist frequency, in cpd:

$$N_f = (1/(\sqrt{3}\, d') \quad (3)$$

where d' is the intercone spacing in degrees, calculated as $d' = d/\mathrm{RMF}$. The estimated Nyquist frequency for the cone mosaic in the central retina of the owl monkey is then 13.7 cpd.

If the cone mosaic indeed imposes the limit for the visual acuity, the owl monkey must have sufficient post-receptoral elements, that is, cone bipolar cells and ganglion cells, in order to preserve the sampling characteristics of the cone array. The peak ganglion cell density in the owl monkey is $\sim 15\,000$ cells/mm^2 (Silveira et al., 1993). If P cells comprise 80%, as in other primates (Perry et al., 1984), these will correspond to about 12 000 cells/mm^2. The resolving power for the P-ON or P-OFF cell mosaic, independently considered, corresponding of a density of 6000 cells/mm^2, would be 8.3 cpd, using the same calculation as above (Eqs. (2)

and (3)). For M cells, the peak density is ~1800 cells/mm^2 (Lima et al., 1996), and the Nyquist frequency for independent M-ON or M-OFF cell mosaics would be 3.2 cpd. Therefore, only the P ganglion cell mosaic in the central retina provides enough sampling elements to account for the owl monkey behaviour visual acuity (Jacobs, 1977), given that a one-to-one connection between cones, bipolar cells and ganglion cells is present.

Currently, the proportion of different types of owl monkey bipolar cells, and particularly, of cone bipolar cells, is unknown. The majority of the midget bipolar cells observed by Ogden (1974) in the owl monkey retina had two sets of dendrites, and thus received inputs from two cones. On the other hand, our results show that the dendritic field diameters of owl monkey P cells, of the order of 15 μm, fall in a similar range of diameters reported by Ogden for axon terminals of midget bipolar cells. Also, the ganglion cell to cone ratio in the same retinal region is close to one-to-one (15 000 ganglion cells/mm^2, Silveira et al., 1993; 16 300 cones/mm^2, present study). Thus, in the nocturnal owl monkey, similarly to what has been reported to diurnal anthropoids (Polyak, 1941; Boycott & Dowling, 1969; Kolb & DeKorver, 1991; Silveira, Lee, Yamada, Kremers, & Hunt, 1998), a one-to-one connectivity might be present in the foveal region, but this assumption has to be confirmed by further studies.

4.3. Rod input to the P pathway

Our results suggest more potential rod input to owl monkey P and M cells than in the diurnal anthropoids such as the capuchin monkey. Weak rod input to macaque and marmoset P pathway has been shown by electrophysiology at the retinal and LGN levels (Yeh et al., 1995; Kremers et al., 1997; Lee, Smith, Pokorny, & Kremers, 1997). Rod pathway input to macaque P cells has been also shown by electron microscopy (Grünert, 1997). Our morphological data show that owl monkey P cells have a much higher potential rod convergence than capuchin monkey P cells, and are more similar to capuchin monkey M cells (Fig. 7C and D). We would thus predict that physiological recordings in the owl monkey will demonstrate a greater amount of rod input to both M and P cells, and that owl monkey P cells might be more similar to M cells, rather than P cells, of diurnal monkeys in this regard. A higher rod convergence has also been reported for the P cells of the bush baby, a nocturnal prosimian (Yamada et al., 1998). Thus, it seems that P cells in nocturnal primates would be better suited to perform at scotopic levels than P cells of diurnal monkeys.

4.4. Cone convergence to ganglion cells

One last point to consider is the striking similarity in cone convergence, in both M and P cells, in the owl monkey and the capuchin monkey. The cone convergence reported here is in the same range as those found in other diurnal and nocturnal primates (Goodchild et al., 1996; Yamada et al., 1998). Why should there be a correlation between cones and ganglion cells? In mammals, retinal neurogenesis occurs in two phases, with most of the cone circuitry being generated in the early phase while the rod circuitry is generated in the late phase (La Vail, Rapaport, & Rakic, 1991). Since ganglion cells and cones are both generated in the first phase, one can argue that the strong correlation between cone density and the size of ganglion cell dendritic fields found across several primate species is not simply coincidental, but the result of specific developmental mechanisms (Goodchild et al., 1996). The fact that nocturnal primates with highly specialized eyes for scotopic vision still kept a 'diurnal pattern' of cone convergence gives further support to this idea. The exact mechanisms involved remain to be determined.

Acknowledgements

This work was supported by FINEP/FADESP 66.94.0034.00, PRONEX/FUJB 76.97.1028.00, CNPq 521640/96-2, and UFPa-PROPESP 20062/93. E.S.Y and L.C.L.S. have CNPq research fellowships. E.C.F. has a CNPq undergraduate fellowship. We thank Professor Barry B. Lee and Dr Jan Kremers for helpful comments on this manuscript. We thank Dr José Augusto P. Muniz, head of the Centro Nacional de Primatas for providing the monkeys used in this study. We thank Cezar Akiyoshi Saito and Francinaldo Lobato Gomes for research assistance.

References

Allman, J. M., & Kaas, J. H. (1971). Representation of the visual field in striate and adjoining cortex of the owl monkey (*Aotus trivirgatus*). *Brain Research*, *35*, 89–106.

Boycott, B. B., & Dowling, J. E. (1969). Organization of the primate retina: light microscopy. *Philosophical Transactions of the Royal Society B* (*London*), *255*, 109–184.

Casagrande, V. A., & Kaas, J. H. (1994). The afferent, intrinsic, and efferent connections of primary visual cortex in primates. In A. Peters, & K. S. Rockland, *Cerebral cortex*, *primary visual cortex in primates*, vol. 10 (pp. 201–259). New York: Plenum Press.

Croner, L. J., & Kaplan, E. (1995). Receptive fields of P and M ganglion cells across the primate retina. *Vision Research*, *35*, 7–24.

Dacey, D. M. (1993). The mosaic of midget ganglion cells in the human retina. *Journal of Neuroscience*, *13*, 5334–5355.

Dacey, D. M., & Petersen, M. R. (1992). Dendritic field size and morphology of midget and parasol ganglion cells of the human retina. *Proceedings of the National Academy of Science of the USA*, *89*, 9666–9670.

de Monasterio, F. M., & Gouras, P. (1975). Functional properties of ganglion cells of the rhesus monkey retina. *Journal of Physiology* (*London*), *251*, 167–195.

Ghosh, K. K., Goodchild, A. K., Sefton, A. E., & Martin, P. R. (1996). Morphology of retinal ganglion cells in a New World monkey, the marmoset *Callithrix jacchus*. *Journal of Comparative Neurology*, *366*, 76–92.

Goodchild, A. K., Ghosh, K. K., & Martin, P. R. (1996). A comparison of photoreceptor spatial density and ganglion cell morphology in the retina of human, macaque monkey, cat, and the marmoset *Callithrix jacchus*. *Journal of Comparative Neurology*, *366*, 55–75.

Gouras, P. (1968). Identification of cone mechanisms in monkey ganglion cells. *Journal of Physiology* (*London*), *199*, 533–547.

Grünert, U. (1997). Anatomical evidence for rod input to the parvocellular pathway in the visual system of the primate. *European Journal of Neuroscience*, *9*, 617–621.

Jacobs, G. H. (1977). Visual capacities of the owl monkey (*Aotus trivirgatus*) — II. Spatial contrast sensitivity. *Vision Research*, *17*, 821–825.

Jacobs, G. H., Deegan, J. F., II, Neitz, J., Crognale, M. A., & Neitz, M. (1993). Photopigments and colour vision in the nocturnal monkey, *Aotus*. *Vision Research*, *33*, 1773–1783.

Jacobs, G. H., Neitz, M., & Neitz, J. (1996). Mutations in S-cone pigment genes and the absence of colour vision in two species of nocturnal primate. *Proceedings of the Royal Society of London*, *Series B*, *Biological Sciences*, *263*, 705–710.

Jones, A. E. (1965). The retinal structure of (*Aotes trivirgatus*) the owl monkey. *Journal of Comparative Neurology*, *125*, 19–28.

Jones, A. E. (1966). Wavelength and intensity effects on the response of single lateral geniculate nucleus units in the owl monkey. *Journal of Neurophysiology*, *29*, 125–138.

Kaas, J. H., & Huerta, M. F. (1988). Subcortical visual system of primates. In H. P. Steklis, & J. Erwin, *Comparative primate biology*, *neurosciences*, vol. 4 (pp. 327–391). New York: Liss.

Kaas, J. H., Huerta, M. F., Weber, J. T., & Harting, J. K. (1978). Patterns of retinal terminations and laminar organization of the lateral geniculate nucleus of primates. *Journal of Comparative Neurology*, *182*, 517–554.

Kaplan, E., & Shapley, R. M. (1982). X and Y cells in the lateral geniculate nucleus of the macaque monkeys. *Journal of Physiology* (*London*), *330*, 125–143.

Kaplan, E., Lee, B. B., & Shapley, R. M. (1990). New views of primate retinal function. In N. N. Osborne, & G. J. Chader, *Progress in retinal research*, vol. 9 (pp. 273–336). Oxford: Pergamon Press.

Kolb, H., & DeKorver, L. (1991). Midget ganglion cells of parafovea of the human retina: a study by electron microscopy and serial-section reconstruction. *Journal of Comparative Neurology*, *303*, 617–636.

Kolb, H., Lindberg, K., & Fisher, S. K. (1992). Neurons of the human retina: a Golgi study. *Journal of Comparative Neurology*, *318*, 147–187.

Kremers, J., & Weiss, S. (1997). Receptive field dimensions of lateral geniculate cells in the common marmoset (*Callithrix jacchus*). *Vision Research*, *37*, 2171–2181.

Kremers, J., Weiss, S., Zrenner, E., & Maurer, J. (1997). Rod and cone inputs to parvo- and magnocellular cells in the dichromatic common marmoset (*Callithrix jacchus*). In C. R. Cavonius, *Colour vision deficiencies*, vol. XIII (pp. 87–97). Dordrecht: Kluwer Academic Publishers.

La Vail, M. M., Rapaport, D. H., & Rakic, P. (1991). Cytogenesis in the monkey retina. *Journal of Comparative Neurology*, *309*, 86–114.

Lee, B. B., Martin, P. R., & Valberg, A. (1988). The physiological basis of heterochromatic flicker photometry demonstrated in the ganglion cells of the macaque retina. *Journal of Physiology* (*London*), *404*, 323–347.

Lee, B. B., Smith, V. C., Pokorny, J., & Kremers, J. (1997). Rod inputs to macaque ganglion cells. *Vision Research*, *37*, 2813–2828.

Lee, B. B, Silveira, L. C. L., Yamada, E. S., Hunt, D. M., Kremers, J., Martin, P. R., Silva-Filho, M., & Troy, J. B. (2000). Visual responses of ganglion cells of a New World primate, the capuchin monkey. *Cebus apella*. *Journal of Physiology (London)* (submitted for publication).

Leventhal, A. G., Rodieck, R. W., & Dreher, B. (1981). Retinal ganglion cell classes in the Old World monkey: morphology and central projections. *Science*, *213*, 1139–1142.

Lima, S. M. A., Silveira, L. C. L., & Perry, V. H. (1996). The distribution of M retinal ganglion cells in diurnal and nocturnal New World monkeys. *Journal of Comparative Neurology*, *368*, 538–552.

Ogden, T. E. (1974). The morphology of retinal neurons of the owl monkey *Aotes*. *Journal of Comparative Neurology*, *153*, 399–428.

Ogden, T. E. (1975). The receptor mosaic of *Aotes trivirgatus*: distribution of rods and cones. *Journal of Comparative Neurology*, *153*, 399–428.

O'Keefe, L. P., Levitt, J. B., Kiper, D. C., Shapley, R. M., & Movshon, A. J. (1998). Functional organization of owl monkey lateral geniculate nucleus and visual cortex. *Journal of Neurophysiology*, *80*, 594–609.

Ordy, J. M., & Samorajski, T. (1968). Visual acuity and ERG-CFF in relation to the morphologic organization of the retina among diurnal and nocturnal primates. *Vision Research*, *8*, 1205–1225.

Peichl, L., & Wässle, H. (1979). Size, scatter and coverage of ganglion cell receptive field centres in the cat retina. *Journal of Physiology* (*London*), *291*, 117–141.

Perry, V. H., & Cowey, A. (1984). Retinal ganglion cells that project to the superior colliculus and pretectum in the macaque monkey. *Neuroscience*, *12*, 1125–1137.

Perry, V. H., Oehler, R., & Cowey, A. (1984). Retinal ganglion cells that project to the dorsal lateral genicuate nucleus in the macaque monkey. *Neuroscience*, *12*, 1101–1123.

Peterson, B. B., & Dacey, D. M. (1999). Morphology of wide-field, monostratified ganglion cells of the human retina. *Visual Neuroscience*, *16*, 107–120.

Polyak, S. L. (1941). *The vertebrate retina*. Chicago, IL: University of Chicago Press.

Purpura, K., Kaplan, E., & Shapley, R. M. (1988). Background light and contrast gain of primate P and M retinal ganglion cells. *Proceedings of the National Academy of Sciences of the USA*, *85*, 534–4537.

Rodieck, R. W., & Watanabe, M. (1993). Survey of the morphology of macaque retinal ganglion cells that project to the pretectum, superior colliculus, and parvicellular laminae of the lateral geniculate nucleus. *Journal of Comparative Neurology*, *338*, 289–303.

Rodieck, R. W., Binmoeller, K. F., & Dineen, J. (1985). Parasol and midget ganglion cells of the human retina. *Journal of Comparative Neurology*, *233*, 115–132.

Rowe, M. H. (1991). Functional organization of the retina. In B. Dreher, & R. R. Robinson, *Vision and visual dysfunction*, *Neuroanatomy of the visual pathways and their development*, vol. 3 (pp. 1–68). Houndmills: Macmillan Press.

Sherman, S. M., Wilson, J. R., Kaas, J. H., & Webb, S. W. (1976). X- and Y-cells in the dorsal lateral geniculate nucleus of the owl monkey (*Aotus trivirgatus*). *Science*, *192*, 475–477.

Silveira, L. C. L., Picanço-Diniz, C. W., Sampaio, L. F. S., & Oswaldo-Cruz, E. (1989). Retinal ganglion cell distribution in the *Cebus* monkey: a comparison with the cortical magnification factors. *Vision Research*, *29*, 1471–1483.

Silveira, L. C. L., Perry, V. H., & Yamada, E. S. (1993). The retinal ganglion cell distribution and the representation of the visual field in area 17 of the owl monkey, *Aotus trivirgatus*. *Visual Neuroscience*, *10*, 887–897.

Silveira, L. C. L., Yamada, E. S., Perry, V. H., & Picanço-Diniz, C. W. (1994). M and P retinal ganglion cells of diurnal and nocturnal New World monkeys. *NeuroReport*, *5*, 2077–2081.

Silveira, L. C. L., Lee, B. B., Yamada, E. S., Kremers, J., & Hunt, D. M. (1998). Post-receptoral mechanisms of colour vision in new world primates. *Vision Research*, *38*, 3329–3337.

Silveira, L. C. L., Yamada, E. S., Franco, E. C. S., & Finlay, B. L. (2000). The specialisation of the owl monkey retina for night vision. *Color Research and Application* (in press).

Solomon, S. G., White, A. J. R., & Martin, P. R. (1999). Temporal contrast sensitivity in the lateral geniculate nucleus of a New World monkey, the marmoset, *Callithrix jacchus*. *Journal of Physiology* (*London*), *517.3*, 907–917.

Usrey, W. M., & Reid, R. C. (2000). Visual physiology of the lateral geniculate nucleus in two species of New World monkey: *Saimiri sciureus* and *Aotus trivirgatus*. *Journal of Physiology* (*London*), *523.3*, 755–769.

Wässle, H., Grünert, U., Röhrenbeck, J., & Boycott, B. B. (1990). Retinal ganglion cell density and cortical magnification factor in the primate. *Vision Research*, *30*, 1897–1990.

Watanabe, M., & Rodieck, R. W. (1989). Parasol and midget ganglion cells. *Journal of Comparative Neurology*, *289*, 434–454.

Webb, S. V., & Kaas, J. H. (1976). The sizes and distribution of ganglion cells in the retina of the owl monkey, *Aotus trivirgatus*. *Vision Research*, *16*, 1247–1254.

Wiesel, T. N., & Hubel, D. H. (1966). Spatial and chromatic interactions in the lateral geniculate body of the rhesus monkey. *Journal of Neurophysiology*, *29*, 1115–1156.

Wikler, K. C., & Rakic, P. (1990). Distribution of photoreceptor subtypes in the retina of diurnal and nocturnal primates. *Journal of Neuroscience*, *10*, 3390–3401.

Yamada, E. S., Silveira, L. C. L., & Perry, V. H. (1996a). The morphology and photoreceptor convergence of *Aotus* M and P retinal ganglion cells. *Abstracts of the ARVO Annual Meeting*, *Fort Lauderdale*, *FL*. *Investigative Ophthalmology & Visual Science*, *37*, S631.

Yamada, E. S., Silveira, L. C. L., & Perry, V. H. (1996b). Morphology, dendritic field size, somal size, density and coverage of M and P retinal ganglion cells of dichromatic *Cebus* monkeys. *Visual Neuroscience*, *13*, 1011–1029.

Yamada, E. S., Marshak, D. M., Silveira, L. C. L., & Casagrande, V. A. (1998). Morphology of P and M retinal ganglion cells of the bush baby. *Vision Research*, *38*, 3345–3352.

Yeh, T., Lee, B. B., Kremers, J., Cowing, J. A., Hunt, D. M., Martin, P. R., & Troy, J. B. (1995). Visual responses in the lateral geniculate nucleus of dichromatic and trichromatic marmosets (*Callithrix jacchus*). *Journal of Neuroscience*, *15*, 7892–7904.